THE ONTARIO WINTER LAKE-EFFECT SYSTEMS FIELD CAMPAIGN

Scientific and Educational Adventures to Further Our Knowledge and Prediction of Lake-Effect Storms

DAVID A. R. KRISTOVICH, RICHARD D. CLARK, JEFFREY FRAME, BART GEERTS, KEVIN R. KNUPP, KAREN A. KOSIBA, NEIL F. LAIRD, NICHOLAS D. METZ, JUSTIN R. MINDER, TODD D. SIKORA, W. JAMES STEENBURGH, SCOTT M. STEIGER, JOSHUA WURMAN, AND GEORGE S. YOUNG

Collaborative field operations in severe winter weather conditions are performed during the OWLeS campaign to observe and understand Great Lakes–generated snow storms.

Snow began to fall on the evening of 17 November 2014, the night before an international headline-making lake-effect snowstorm. Less than two days later, more than 150 cm of snow covered parts of Buffalo, New York; roofs had collapsed; thousands of motorists were stranded; and power went out from falling trees and branches (NWS 2015). Much of the same region was blanketed by up to an additional 125 cm over the following three days (19–21 November 2014).

The November 2014 Buffalo storms provide an example of the frequent, sometimes intense, lake-effect snowstorms produced by the Great Lakes of North America during the cool season (e.g., Niziol et al. 1995). The area to the east of Lake Ontario in particular experiences some of the most intense snowstorms in the world. High snowfall rates, low visibility, and heavy accumulations have large impacts on businesses, transportation, and health systems in regional communities. Lake-effect snowstorms, however, benefit some economic sectors such as building supply and snow removal businesses and a vibrant winter-sports economy (Schmidlin 1993; Kunkel et al. 2002; Tug Hill Commission 2015). Many lake-effect

AFFILIATIONS: KRISTOVICH—Illinois State Water Survey, Prairie Research Institute, University of Illinois at Urbana–Champaign, Champaign, Illinois; CLARK AND SIKORA—Department of Earth Sciences, Millersville University, Millersville, Pennsylvania; FRAME—Department of Atmospheric Sciences, University of Illinois at Urbana–Champaign, Champaign, Illinois; GEERTS—Department of Atmospheric Sciences, University of Wyoming, Laramie, Wyoming; KNUPP—University of Alabama in Huntsville, Huntsville, Alabama; KOSIBA AND WURMAN—Center for Severe Weather Research, Boulder, Colorado; LAIRD AND METZ—Department of Geoscience, Hobart and William Smith Colleges, Geneva, New York; MINDER—Department of Atmospheric and Environmental Sciences, University at Albany, State University of New York, Albany, New York; STEENBURGH—Department of Atmospheric Sciences, University of Utah, Salt Lake City, Utah; STEIGER—Department of Atmospheric and Geological Sciences, State University of New York at Oswego, Oswego, New York; YOUNG—Department of Meteorology, The Pennsylvania State University, University Park, Pennsylvania
CORRESPONDING AUTHOR E-MAIL: David Kristovich, dkristo@illinois.edu

The abstract for this article can be found in this issue, following the table of contents.
DOI:10.1175/BAMS-D-15-00034.1

In final form 24 May 2016

snowstorms are enhanced over the Tug Hill Plateau (hereafter Tug Hill; Fig. 1), which rises ~500 m above lake level. Record snowfall accumulations observed in this region of New York include 30.5 cm in 1 h at Copenhagen, 44.5 cm in 2 h at Oswego, and 129.5 cm in 16 h at Bennetts Bridge (Burt 2007).

To better understand and improve forecasts of intense lake-effect storms, the Ontario Winter Lake-effect Systems (OWLeS) project was conducted over a 2-month period spanning December 2013 and January 2014. An extensive array of instrumentation was deployed via funding from the National Science Foundation to understand processes ranging from the microphysical evolution of lake-effect clouds and snow to lake-scale circulation patterns that organize the convection into coherent bands. This article describes the OWLeS scientific objectives and data-collection strategies, initial findings, and lessons learned in conducting a field project in some of the worst winter weather observed in North America.

SCIENTIFIC OBJECTIVES AND DESIGN.

The OWLeS project was organized around three major components: 1) surface and atmospheric influences on lake-effect (SAIL) convection, which focused on the response of atmospheric flow over varying land, water, and ice surfaces; 2) long-lake-axis-parallel (LLAP) snow systems, associated with some of the most intense snowfalls in the eastern Great Lakes; and 3) interactions between lake-effect systems (LeS) and Tug Hill east of Lake Ontario. These complementary components provided an opportunity to enhance the understanding and prediction of lake-effect snowstorms.

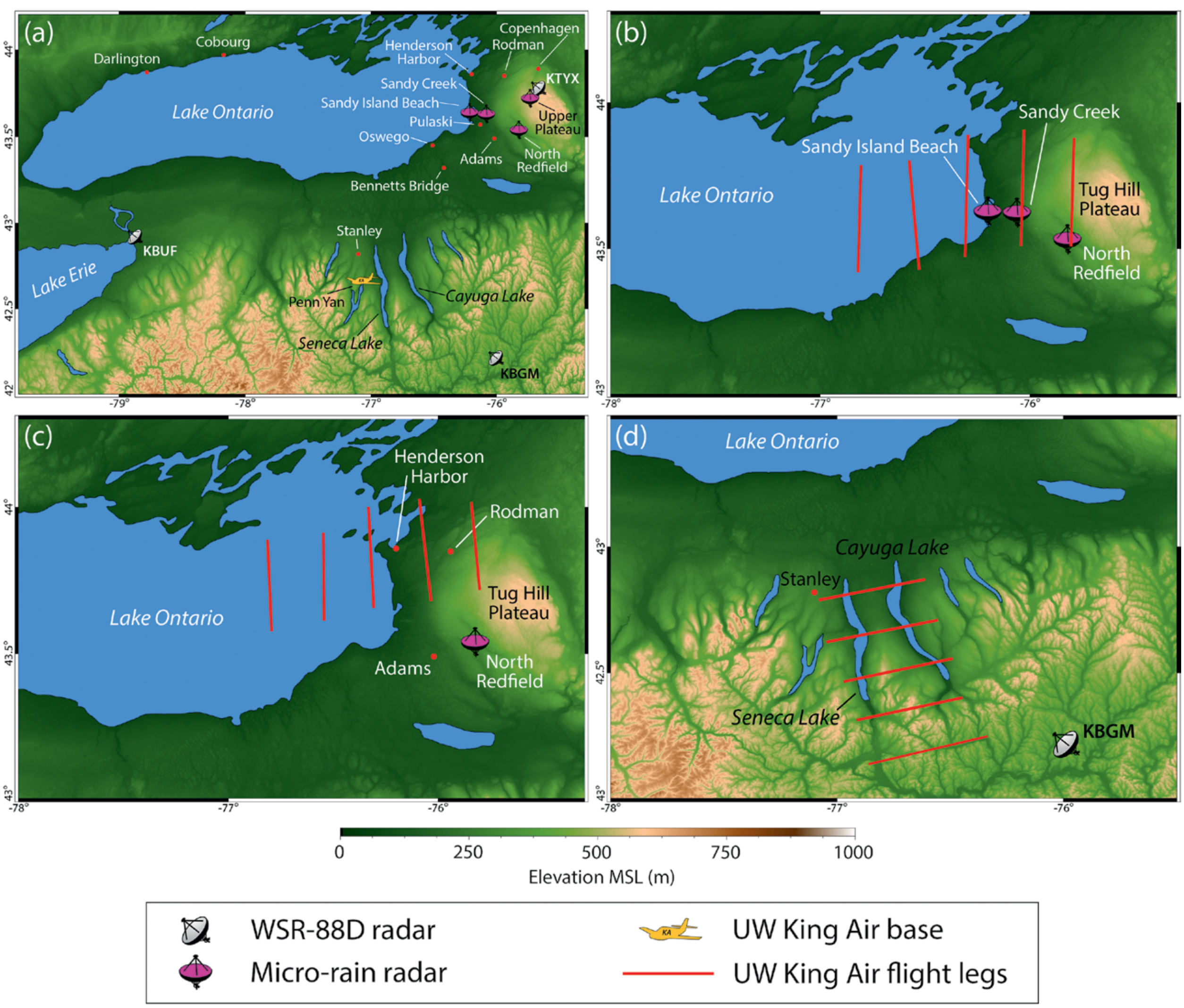

Fig. 1. (a) Map showing all deployment locations discussed in this manuscript. Examples of facility deployment during (b) IOP 2b (intense LLAP snowband), (c) IOP 7 (intense LLAP snowband), and (d) IOP 17 (Finger Lakes snowbands). WCR data from the middle flight leg shown in (b) are plotted in Fig. 3.

Specifically, the scientific goals related to OWLeS research are to 1) understand the development of, and interactions between, internal planetary boundary layers (PBLs) and residual layers resulting from advection over multiple mesoscale water bodies and intervening land surfaces; 2) understand the processes involved in the development of lake-effect snows over the New York State Finger Lakes and how these processes differ from the larger Great Lakes; 3) examine how organized, initially convective lake-effect structures persist far downstream over land, long after leaving the buoyancy source; 4) examine how surface fluxes, lake-scale circulations, cloud microphysics, and radiative processes affect the formation and structure of long-fetch LeSs; 5) understand the dynamical and microphysical processes controlling the finescale kinematic structures and electrification processes of intense long-fetch LeSs; 6) provide in situ validation of operational (S band) and research (X band) dual-polarization hydrometeor type classification and lake-effect snowstorm QPE; and 7) understand the influence of downwind topography on LeSs generated over Lake Ontario.

A large number of advanced observational facilities were deployed during intensive observation periods (IOPs) to gain an unprecedented dataset on LeSs (Table 1). Many of the common locations for the surface-based facilities during IOPs are shown in Fig. 1a; aircraft flight patterns are illustrated in Figs. 1b–d. Observations collected by these facilities, as well as those taken operationally in the United

Table 1. Major observational platforms deployed during the OWLeS field operations.

ID	Platform	Owner/operator	Location	Reference
A	UWKA	NSF facility, UW	Mobile	www.atmos.uwyo.edu/n2uw/
B	Wyoming Cloud Radar	NSF facility, UW	Mobile	Pazmany et al. (1994)
C	Wyoming Cloud Lidar	NSF facility, UW	Mobile	Wang et al. (2012)
D	DOW 6 and DOW 7	NSF facility, CSWR	Mobile	Wurman et al. (1997); Wurman (2002)
E	DOW 8 (rapid scan)	NSF facility, CSWR	Mobile	Bluestein et al. (2010)
F	MUPS (wide range of observations)	MU	Mobile	www.millersville.edu/esci/maraf/index.php
G	MIPS (wide range of observations)	UAH	Mobile	http://vortex.nsstc.uah.edu/mips/system/
H	Radiosonde sounding systems	HWS, MU, SUNY-O, UIUC, UU	Mobile	
I	iMet rawinsonde/anasphere liquid water sonde	NCAR/RAL, NASA	Oswego	
J	Hydrometeor videosonde (HYVIS) snow crystal camera	UU	North Redfield	
K	MRRs (4)	UU, SUNY-A	Sandy Island Beach State Park, Sandy Creek Central School, private residences north of Redfield, and on upper Tug Hill	Peters et al. (2002); Maahn and Kollias (2012)
L	North Redfield Snow Study Station (meteorological variables, snow depth, camera)	UU	North Redfield	
M	Sandy Creek Snow Study Station (meteorological variables, snow depth, camera)	UU	Sandy Creek	
N	UW Hotplate (snowfall)	UW	North Redfield	
O	Mobile surface snow observations	SUNY-O	Mobile	
P	CSWR weather Pod	CSWR	Mobile	

States and Canada, have been integrated, quality controlled, and archived at the UCAR Earth Observing Laboratory (www.eol.ucar.edu/field_projects/owles).

SAIL convection. Observational and associated numerical weather prediction studies have revealed much about the complex evolution of LeSs and examined the broader issues of atmospheric convective PBL responses, mesoscale circulations, and microphysical processes that are associated with variations in surface properties (e.g., Agee and Hart 1990; Braham 1990; Hjelmfelt 1990; Chang and Braham 1991; Rao and Agee 1996; Braham and Kristovich 1996; Kristovich and Braham 1998; Kristovich and Laird 1998; Kristovich et al. 1999; Young et al. 2000; Laird et al. 2001; Young et al. 2002; Kristovich et al. 2003; Laird et al. 2003; Miles and Verlinde 2005; Schroeder et al. 2006; Yang and Geerts 2006; Cordeira and Laird 2008; Steiger et al. 2009; Laird et al. 2009; Alcott et al. 2012). This previous work has raised a number of important scientific questions:

1) How do multiple internal boundary layers develop and interact as an air mass progresses over multiple mesoscale stretches of open water and intervening land or ice?
2) What effect does the variation in these multiple internal boundary layers have on the circulation patterns, longevity, and intensity of lake-effect snowstorms?
3) How does the interplay between dynamics and mixed-phase cloud processes produce long-lived LeSs persisting far downwind of open water?
4) How are PBL circulations and lake-effect snowstorm intensity affected by coastal transitions? The key objectives of the SAIL IOPs were to take observations during lake-effect conditions, including cases when there was evidence of cold air consecutively crossing more than one lake, which allowed for a better understanding of these boundary layer processes in LeS situations.

During most SAIL IOPs, the University of Wyoming (UW) King Air (UWKA) research aircraft flew stacks of straight and level flight legs at various heights within and above the PBL, approximately perpendicular to the mean boundary layer wind direction. Those observations, together with those from various combinations of mobile sounding systems, vertical profiling systems, and Doppler on Wheels radars (DOWs) provided the opportunity to better understand the evolution of the boundary layer, clouds, precipitation, and circulation patterns from over the lake surface to far downwind. Since SAIL events were not limited to LLAP band cases and frequently exhibited snowfall over large regions downwind of Lakes Erie and Ontario, data for multiple objectives were often sought simultaneously.

LLAP snow systems. Singular zonal LLAP snowbands occasionally form over Lake Ontario when the low-level wind aligns with the lake's long axis (Niziol et al. 1995; Veals and Steenburgh 2015). These events were unusually common during OWLeS, with 12 IOPs focused on LLAP systems, compared to the two to three events typically seen over Lake Ontario during the December–January period (Rodriguez et al. 2007). The key objectives of the LLAP IOPs were to examine the finescale cloud and dynamical processes in LLAP systems, including occasional lightning; to investigate how LLAP systems intensify and evolve downwind of the lake; and to discover how radar dual-polarization variables at both X and S bands reveal precipitation processes in LeSs.

Figures 1b and 1c show examples of facilities deployment for LLAP objectives. The UWKA flew a lawnmower pattern across the LLAP band, starting with offshore transects, followed by onshore transects often extending over Tug Hill. In some cases the aircraft also flew along and within the LLAP band, including as far east as the Adirondacks for two IOPs, to examine the evolution of vertical velocity and cloud processes. Two or three DOWs were usually positioned along or near the eastern shore of Lake Ontario (not shown) to collect data for multiple Doppler wind analysis. The preferred Mobile Integrated Profiling System (MIPS) location was under the LLAP band. In several IOPs, the band slowly passed over the MIPS. Soundings were released from the upwind shore and downwind from the lake within, north, and south of the band. Snow crystals were imaged from up to three surface locations in or near the band. Two mesonet vehicles distributed weather Pods, rapidly deployable ruggedized platforms for collecting standard meteorological observations of temperature, relative humidity, wind velocity, and pressure at several heights (www.cswr.org/contents/mesonets&PODs.php), in transects across the band, when weather permitted.

OWLeS-Orographic. Lake-effect and related systems are strongly influenced by orography of all scales from the low hills of Michigan (Hjelmfelt 1992) to the high mountains downstream of the Great Salt Lake and the Sea of Japan (Magono et al. 1966; Saito et al. 1996; Kusunoki et al. 2004; Yeager et al. 2013; Alcott and Steenburgh 2013). Rising with a shallow, quasi-continuous ~1.25% slope to ~500 m above Lake Ontario, Tug Hill of northern New York experiences some of the most intense snowstorms on Earth and observes a mean annual snowfall of over 700 cm, making it the snowiest region in the northeast United States (Burt 2007; Veals and Steenburgh 2015).

The OWLeS-Orographic component examines precipitation enhancement over Tug Hill during LLAP events. Field operations focused on an "orographic transect" of four observing stations in New York from the eastern shore of Lake Ontario to upper Tug Hill (Fig. 1a): 1) Sandy Island Beach on the east shore; 2) Sandy Creek, New York, at the base of Tug Hill; 3) North Redfield, New York, which is likely the snowiest car-accessible location on the western slope of Tug Hill (Veals and Steenburgh 2015); and 4) the upper plateau.

Vertically profiling 24-GHz METEK Micro Rain Radar 2 (MRR) Doppler radar systems (Peters et al. 2002; Maahn and Kollias 2012) operated continuously at all four sites during most of the field project, with a period of collocated operation for calibration in North Redfield during late January. Automated meteorological and snow measurement stations were operated in wind-protected sites in Sandy Creek and North Redfield and were supplemented with 6-hourly manual snow observations during and around IOPs to enable quantification of snowfall intensity (amount and liquid precipitation equivalent). During several LLAP IOPs, the UWKA flew over the orographic transect, further enhancing data collection for investigations of orographic influences. Sandy Creek frequently served as the base for other mobile facilities [e.g., the Millersville University (MU) Profiling System (MUPS) and MIPS], while sounding and snow crystal observations were taken concurrently at North Redfield.

FIELD OPERATIONS. The winter of 2013/14 offered an abundance of lake-effect snowstorms in association with below-normal temperatures and resulted in above-normal snowfall across much of the Great Lakes region (MRCC 2015; NRCC 2015). Overall, 24 IOPs were conducted during OWLeS, some of which lasted multiple days. Table 2 provides a list of the IOPs and project foci; more comprehensive IOP information can be found online (http://catalog.eol.ucar.edu/owles/tools/missions). On average, OWLeS IOPs occurred every 1.6 days (taking into account overlapping IOPs). The next section describes field operations from several events.

IOP 2b: A major LLAP system event. IOP 2b occurred during a 2-day period of lake-effect snow that produced the largest storm-total (117.0 cm) and 24-h (101.5 cm) snowfall accumulations observed at North Redfield during the field campaign (measurements based on the average of manual measurements collected from two snowboards). Snowfall rates were prodigious, with 33 cm falling from 1800 UTC 11 December through 0000 UTC 12 December. Hourly accumulations based on automated sensors exceeded 10 cm at times. Based on 6-h manual measurements, the mean snow-to-liquid ratio for the event was 17:1.

Strong and unusually deep (about 3 km, compared to the more common 1–2 km deep) LLAP bands developed at times during this IOP. Radar-estimated precipitation during the period of largest 24-h accumulation (0000 UTC 11 December–0000 UTC 12 December) featured an elongated maximum centered over the orographic transect (location in Fig. 1a) with liquid precipitation equivalent increasing from eastern Lake Ontario to a broad maximum over Tug Hill (Minder et al. 2015, their Fig. 4). Manually observed snowfall (liquid precipitation equivalent) based on the average of manual 6-h measurements taken on two snowboards at each site increased from 47.8 cm (33.5 mm) at Sandy Creek to 101.5 cm (62.5 mm) at North Redfield. The resulting enhancement factor was 2.1 (1.9), with an elevation increase of only ~250 m.

Significant changes in cloud-scale structures occurred from the coast to Tug Hill (Minder et al. 2015; Campbell et al. 2016). MRR-observed reflectivity was highly variable in time and sometimes exceeded 25 dB*Z* at Sandy Island Beach with echoes extending to the capping inversion at ~3 km MSL (Fig. 2a). Despite larger total snowfall, echo-top heights at North Redfield were comparable and maximum reflectivities were lower (Fig. 2b). However, less temporal variability was observed, resulting in more continuous snowfall (Minder et al. 2015). UWKA cloud radar observations collected during a strong LLAP band period reveal a transition from vigorous updrafts and downdrafts near the coast to stratiform ascent with shallow near-surface boundary layer turbulence over the western slope of Tug Hill.

IOP 7: LLAP system event. On 7 January 2014, the coldest Arctic air of the winter season to that point (surface air temperatures ranging from −19° to −10°C) moved southward over the Great Lakes region, setting the stage for a prolific (see sidebar discussing the extreme snowfalls during OWLeS) and long-lived lake-effect snowstorm over and downwind of Lake

Table 2. IOPs during OWLeS. LLAP represents long-lake-axis parallel snowband cases, SAIL represents surface and atmospheric influences on lake-effect cases, and orographic denotes studies of lake-effect interactions with Tug Hill.

IOP	Duration	Type of event	Platforms deployed (see Table 1)
1	1600–2300 UTC 7 Dec	LLAP	A, B, C, G, H, J, K, L, M, O, P
2a	1639–2018 UTC 10 Dec	SAIL	A, B, C, G, F, H, J, K, L, M, N, O, P
2b	2300 UTC 10 Dec–0200 UTC 12 Dec	LLAP	A, B, C, G, F, H, J, K, L, M, N, O, P
3	2100 UTC 12 Dec–0700 UTC 13 Dec	LLAP	A, B, C, G, H, J, K, L, M, N, O, P
4	2040 UTC 15 Dec–0700 UTC 16 Dec	LLAP	A, B, C, D, E, F, G, H, J, K, L, M, N, O, P
5	1600 UTC 18 Dec–0000 UTC 19 Dec	LLAP	D, E, F, G, H, J, K, L, M, N, O
6	1700–2200 UTC 6 Jan	SAIL	A, B, C, D, E, H, J, K, L, M, N
7	2100 UTC 6 Jan–2230 UTC 7 Jan	LLAP	A, B, C, D, E, F, G, H, J, K, L, M, N, O
8	1400–2200 UTC 8 Jan	SAIL	A, B, C, F, H, K, L, M, N
9	0100–1600 UTC 9 Jan	LLAP	A, B, C, D, E, F, G, H, I, K, L, M, N, O
10	1100–1530 UTC 12 Jan	Orographic	A, B, C, D, H, J, K, L, M, N
11*	2300 UTC 15 Jan–0400 UTC 16 Jan	SAIL	F, H, K, L, M, N
13	2200 UTC 18 Jan–0300 UTC 19 Jan	LLAP	A, B, C, F, G, K, L, M, N
14	2100 UTC 19 Jan–0200 UTC 20 Jan	Orographic	A, B, C, D, G, H, J, K, L, M, N, O
15	0500–1200 UTC 20 Jan	LLAP	D, E, G, H, K, L, M, N, O
16	1700 UTC 20 Jan–0000 UTC 22 Jan	SAIL	A, B, C, D, E, H, K, L, M, N
17	1200–1700 UTC 22 Jan	SAIL	A, B, C, D, F, H, K, L, M, N
18	1700 UTC 23 Jan–0300 UTC 24 Jan	SAIL	A, B, C, D, F, H, K, L, M, N, P
19	0500–1400 UTC 24 Jan	LLAP	D, F, K, L, M, N
20	1200–2000 UTC 26 Jan	SAIL	A, B, C, D, F, G, H, K, L, M, N
21	1600 UTC 27 Jan–0000 UTC 28 Jan	SAIL	A, B, C, D, F, G, H, J, K, L, M, N
22	2300 UTC 27 Jan–1900 UTC 28 Jan	LLAP	D, E, G, H, J, K, L, M, N
23	1500–2130 UTC 28 Jan	SAIL	A, B, C, D, F, G, H, K, L, M, N
24	1700–1930 UTC 29 Jan	LLAP	A, B, C, H, K, L, M, N

*There is no IOP 12.

Ontario. The event began as multiple bands streaming off the eastern end of Lake Ontario that consolidated into a single LLAP band extending from central into northeastern Lake Ontario and downwind land areas as a vigorous short-wave trough traversed over Lake Ontario. A sharp reflectivity gradient with a line of misovortices (small-scale vortices with sizes on the order of 0.1–1 km) was evident along the northern edge of this band. The Earth Networks Total Lightning Network (ENTLN) detected a total of 24 lightning flashes well inland between 0630 and 1130 UTC. This case is discussed in more detail below.

Two DOWs operated for more than 20 h near the eastern shore of Lake Ontario to collect data near the location where the snowband reached the shoreline. Their positions allow for a large area of dual-Doppler wind field analyses. The third DOW operated farther inland to observe the snowband evolution over Tug Hill. The UWKA conducted transects across this intense LLAP snowband while most other facilities operated within or near the snowband throughout the 25.5-h IOP.

IOP 17: Finger Lakes LeS event. Much of the current knowledge regarding lake-effect snowstorms has been developed through investigations of systems associated with large water bodies, such as Lake Ontario. Lake-effect snowfalls and mesoscale circulations associated with smaller lakes have received less attention. The Finger Lakes are capable of producing lake-effect snows despite the two largest lakes in the region, Seneca and Cayuga, being only 5 km wide (Laird et al. 2009, 2010). Both lakes produced lake-effect snowbands over the multiday period of 20–22 January 2014, when the wind aligned with their 60-km-long axes. Typically, Finger Lakes lake-effect snowstorms occur for durations of less than 12 h

EXTREME SNOWFALLS DURING OWLES

OWLeS field operations occurred during a remarkably active lake-effect period. During the December 2013–January 2014 period, an NWS spotter in North Redfield recorded 649 cm of snowfall compared to 13-yr means of 402 cm. During operations for the December IOPs (1–5), OWLeS scientists recorded 244.5 cm of snow with maximum storm, 24-h, and 6-h accumulations of 117.0 cm (IOP 2b), 101.5 cm (IOP 2b), and 36.3 cm (IOP 4), respectively, based on the average of manual measurements from two snowboards. Automated snow-depth sensors recorded maximum snowfall rates greater than 10 cm h^{-1} during IOPs 2b, 3, and 4 at North Redfield and during IOPs 2b and 4 at Sandy Creek. Much of this snow was remarkably dry with high snow-to-liquid ratios. For example, during operations for December IOPs, the average snow-to-liquid ratio at North Redfield was 17:1.

The 6–8 January 2014 snowstorm examined during IOPs 6/7 produced the largest storm total accumulations of the campaign with 123 cm in Adams, New York, and 152.5 cm in Rodman, New York. Snowfall rates reached as high as 9 cm h^{-1}, with wind gusts of over 15 m s^{-1} creating significant drifting snow with near-white-out conditions at times. These extreme conditions, combined with temperatures as low as −17°C at low elevations and −20°C on Tug Hill, created the most challenging operational conditions of the field campaign.

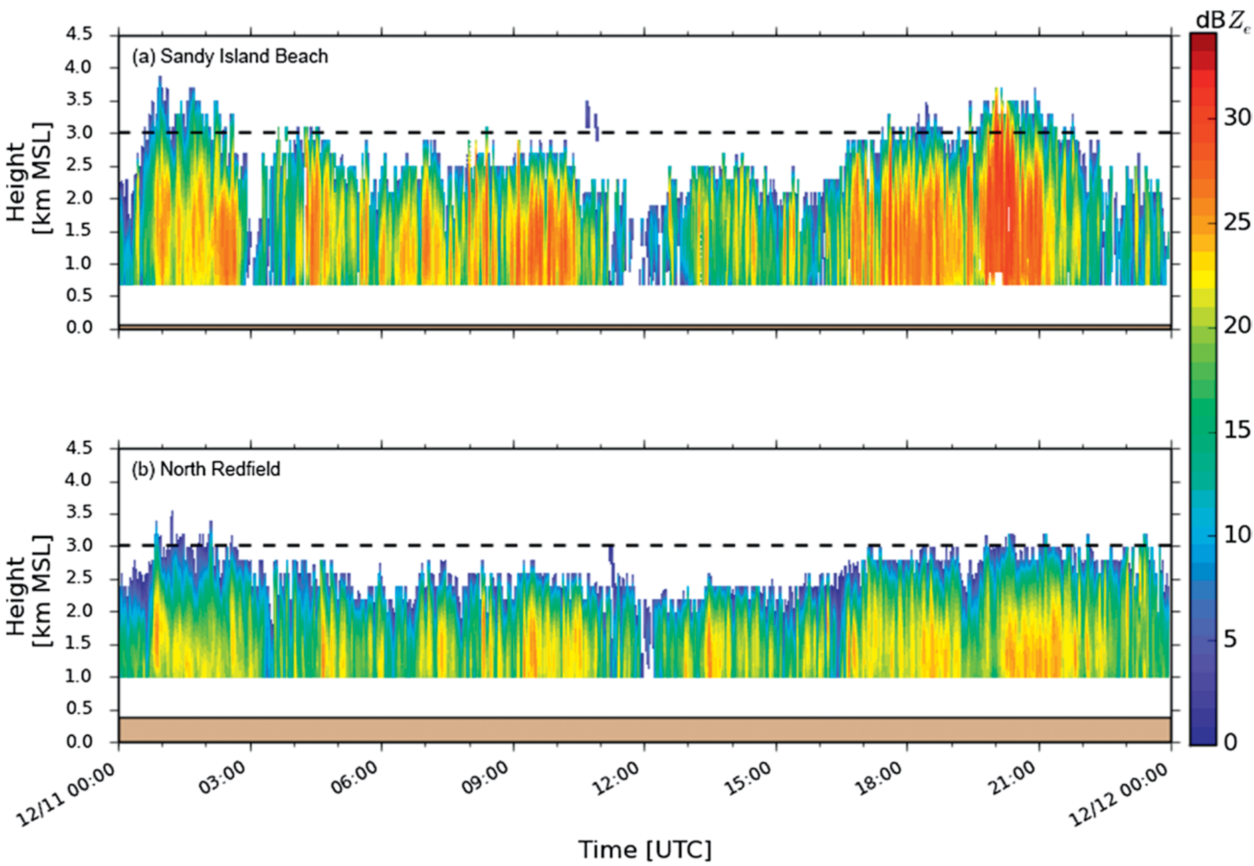

Fig. 2. Time–height plot of the equivalent radar reflectivity factor Z_e measured by MRR profiling radars during IOP 2b at (a) Sandy Island Beach and (b) North Redfield. Heights below ground level at each site are shaded in tan. Data are unavailable in the lowest few 100 m above ground. The dashed black line shows the 3 km MSL height for reference. This figure is adapted from Minder et al. (2015, their Fig. 6).

(Laird et al. 2009); OWLeS investigations benefited from this exceptionally long-duration event (nearly 48 h). This event featured a variety of subtle changes in wind speed, direction, and other atmospheric variables, which resulted in varying locations and intensities of lake-effect snowbands over Seneca and Cayuga Lakes. At times the convection was intense enough to produce waterspouts. During one of the lake-effect periods, the UWKA flew a series of crosswind transects over both lakes from the upwind northern side to the higher terrain downwind (south) of the lakes (see Fig. 1d). Snow and liquid water were present very early in the first convective clouds that developed over the lakes, near their upwind shores. Farther downwind, the UWKA in situ probes and Wyoming Cloud Radar (WCR) dual-Doppler analysis showed a solenoidal circulation pattern with near-surface convergence over each lake, buoyant updrafts about 1 km deep, and divergence aloft (Bergmaier and Geerts 2016). Near the downwind shores light snowfall became more widespread as a result of orographic ascent and band interactions with more complex terrain.

OBSERVED PROCESSES AND PHENOMENA.

Mesoscale band circulation patterns. Previous studies have found that surface buoyant forcing over the relatively warm waters of Lake Ontario, produced by surface vertical sensible and latent heat fluxes (Drennan et al. 2007; Byrd et al. 1991) and the upward distribution of heat over the depth of the lake-effect convection, is likely to produce a solenoidal circulation pattern over the width of the lake. This may explain past observations of the collapse of multiple wind-aligned lake-effect snowbands into a single LLAP band (Ballentine et al. 1998). However, the cross-lake structures of the precipitation and circulation patterns have rarely been observed.

A flight transect across the IOP 2b LLAP band near the east end of Lake Ontario (Fig. 3) reveals a deep, 10 m s^{-1} strong updraft, far narrower than the LLAP band itself. Flight-level data at lower levels (not shown) do not reveal significant buoyancy, but a 1–2-K isobaric temperature difference did exist across the width of the transect, concentrated at the core updraft, with the colder air to the north. Snow is lofted by the strong updraft, producing the prominent LLAP band (Fig. 3). The main updraft is consistent with very shallow convergent flow from opposite sides of the lake, strongest from the north in this case, and deep upper-level divergence evident in the streamlines and the reflectivity field. A variety of other smaller-scale features are evident as well. Some of these are examined below and in Welsh et al. (2016).

Misocyclones and related phenomena. Small-scale vortices on the order of 0.1–1 km in sea- and lake-effect storms have been documented over the Sea of Japan

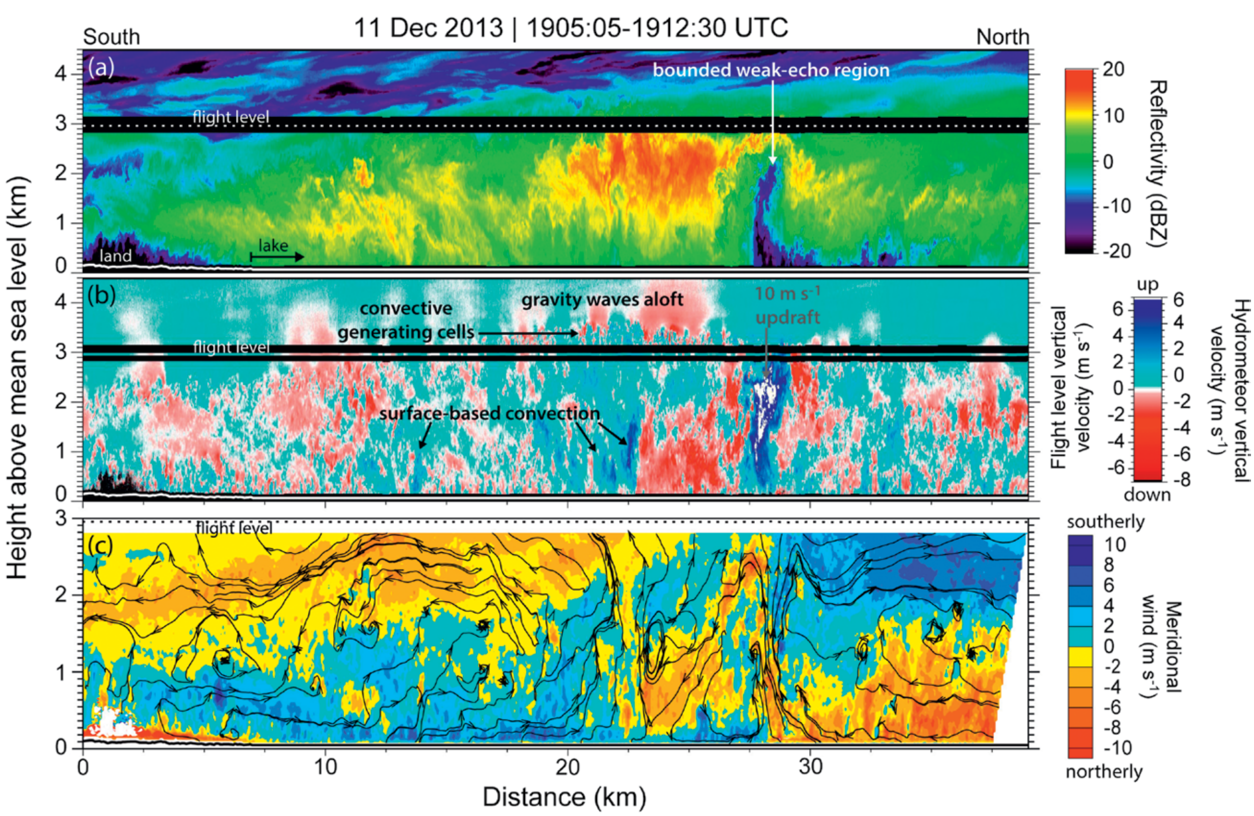

FIG. 3. Meridional transect of WCR data across the IOP 2 LLAP band along the middle flight leg shown in Fig. 1b: (a) reflectivity; (b) hydrometeor vertical velocity; (c) 2D flow streamlines and along-track (meridional) wind speed v', defined as $v' = v - \bar{v}(z)$, where v is the WCR-retrieved along-track wind, and $\bar{v}(z)$ is the mean value as a function of height z. Note that the vertical velocity scale in (b) is offset and centered at −1 m s^{-1}, to account for the fall speed of (unrimed) snow; thus, the color field can be interpreted as updrafts in blue and downdrafts in red.

(Inoue et al. 2011) and over Lake Ontario (Steiger et al. 2013). However, while these studies have documented the existence of small-scale vortices, the evolution of their finescale three-dimensional kinematics has yet to be investigated. DOWs (Wurman et al. 2014) deployed during OWLeS provided observations to investigate the frequency and persistence of these vortices, their structure and evolution, and their relationship to snowband intensity, morphology, and microphysics.

Of 12 OWLeS LLAP events, 11 of them contained bands with small-scale vortical features, often organized in a line (Fig. 4). The life spans of these lines of vortices commonly were 1–3 h. Vortices were observed on the north and south sides and internally to the bands. These vortices likely formed on convergence lines (e.g., Kosiba et al. 2014), as shown in preliminary dual-Doppler analysis of the evolution of a line of vortices from IOP 4 (K. Kosiba et al. 2016, unpublished manuscript).

Lake-effect lightning. At least six lake-effect lightning events occurred during the OWLeS field campaign (see video of lightning by one of the OWLeS student field teams online: www.youtube.com/watch?v=KXRe7npyw4Q). Two of the most significant lightning events occurred during IOPs 5 and 7. During IOP 5 (7), there were 2 (11) human lightning/thunder reports and 5 (24) flashes detected by the ENTLN. Flash rates approached five flashes per hour in each event. December is a climatologically favored period for lake-effect lightning (Steiger et al. 2009) and environmental conditions supported electrification in IOP 5 (e.g., warmer boundary layer, the MIPS Microwave Profiling Radiometer maximum liquid water path values were 1.95 versus 0.24 mm in IOP 7,

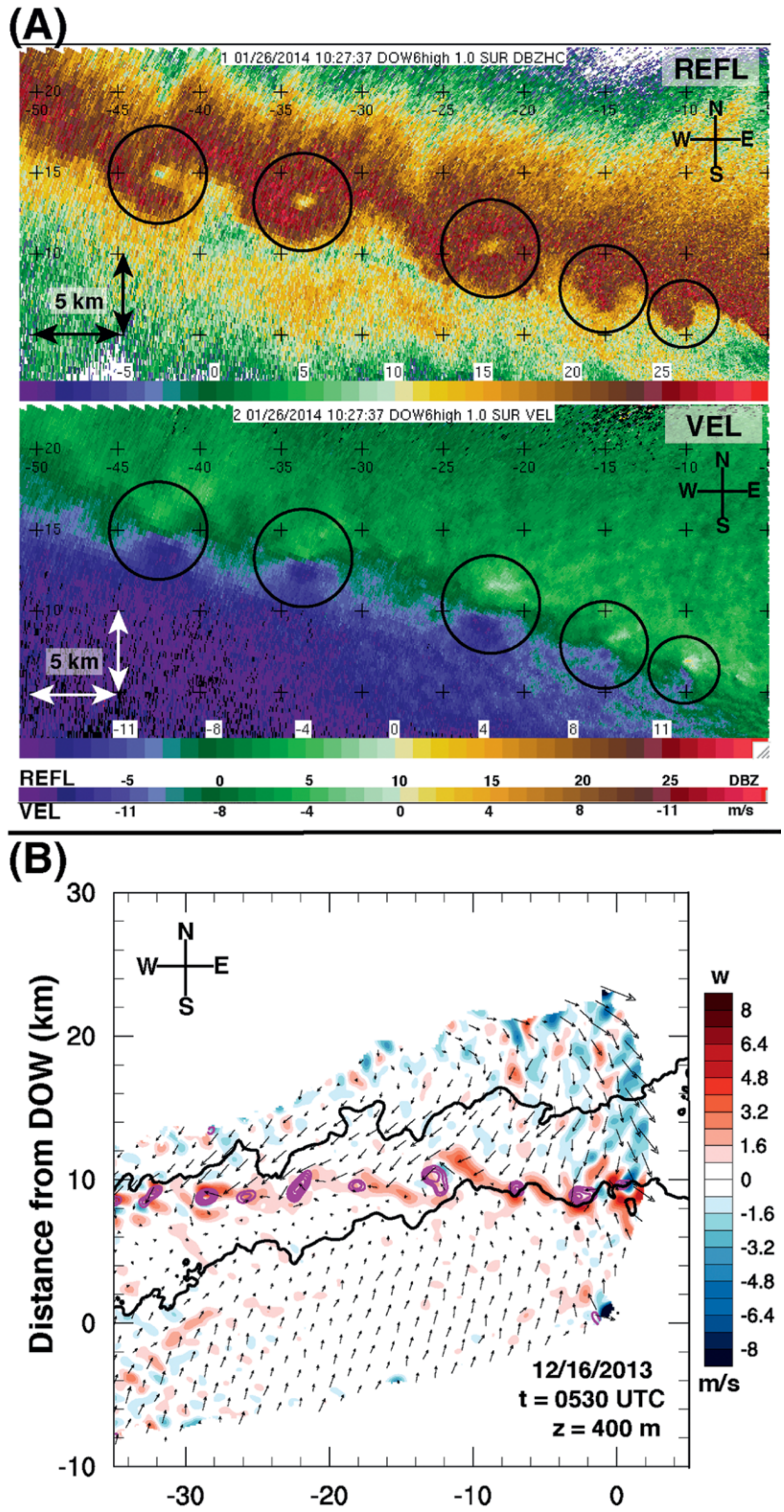

Fig. 4. DOW observations of misoscyclones in LLAP lake-effect snowbands. (a) The reflectivity and Doppler velocity of a band observed on 26 Jan 2014 (IOP 20). Black circles indicate locations of misocyclones. (b) Dual-DOW synthesis of misoscyclones from a band observed on 16 Dec 2013 (IOP 4). Vectors depict the band-relative horizontal winds, color contours depict vertical motion, black contour is the 20-dBZ isopleth, and magenta contours indicate vertical vorticity (from Kosiba et al. 2016, unpublished manuscript).

many surface graupel reports), yet IOP 7 was much more electrically active. The MIPS X-band Profiling Radar (XPR) showed many more strong updrafts over land (approaching 8 m s^{-1}) in the snowband cells during IOP 5. However, cloud depths were 0.5 km greater in IOP 7 and the lake-induced buoyant instability calculated using upwind radiosonde and mean lake surface temperature data (method described in Minder et al. 2015) was near 1300 J kg^{-1} (more than 4 times larger than in IOP 5). Many of the lightning strikes in both events occurred near a wind farm of nearly 200 turbines on Tug Hill.

Microphysical features. During the OWLeS field campaign, two of the three DOWs deployed were dual-polarization systems (DOW6 and DOW7; Wurman et al. 2013), which allowed for radar measurement of the evolution of snow crystals and graupel. Paired with data from the UWKA, surface snow crystal imaging, and dual-Doppler wind syntheses, the coevolution of the snow microphysics and kinematics was documented in unprecedented detail.

Numerous proximity soundings provided vertical thermodynamic data for hydrometeor classification algorithms. When the X-band (3-cm wavelength) DOWs were deployed along the east and east-southeast coast of Lake Ontario, contemporaneous data from the dual-polarization S-band (10-cm wavelength) Weather Surveillance Radar-1988 Doppler (WSR-88D) radar in Montague, New York (KTYX), permitted comparisons between dual-polarization fields and particle identification schemes.

Inland convective transition of lake-effect plumes. Boundary layer convection is a frequent occurrence within the aggregate plume of destabilized and moistened air downwind of the Great Lakes (e.g., Sousounis and Fritsch 1994). The resulting fields of shallow cumulus, arranged as either cells or rolls, typically produce light precipitation in the form of snow flurries. Some events, however, result in cumulus congestus clouds that produce intense snow squalls. OWLeS sampled this overland convection within the aggregate plume using the UWKA, MUPS, and DOWs. UWKA in situ and cloud radar observations reveal that this overland convection is much stronger than would be driven by such relatively weak surface heat fluxes alone—usually less than 50 W m^{-2}. A potential explanation for the strong overland convection is suggested by the preferential occurrence of overland convection during cold-air advection. Cold air may move across the land areas near the top of the boundary layer more quickly than near the surface, resulting in destabilization of the layer. Yet, surface forcing (Fig. 5) does play some role, as this overland convection is primarily a daytime phenomenon. Thus, surface layer stability is suggested as a modulating factor for friction and thus an advectively driven boundary layer destabilization process. The term boundary layer is used here to refer to both the cloud and subcloud layers, as they are convectively coupled into a joint mixed layer during lake-effect events.

Analyses are under way to explore the relationship between overland convection and boundary layer stability change processes within the lake-aggregate

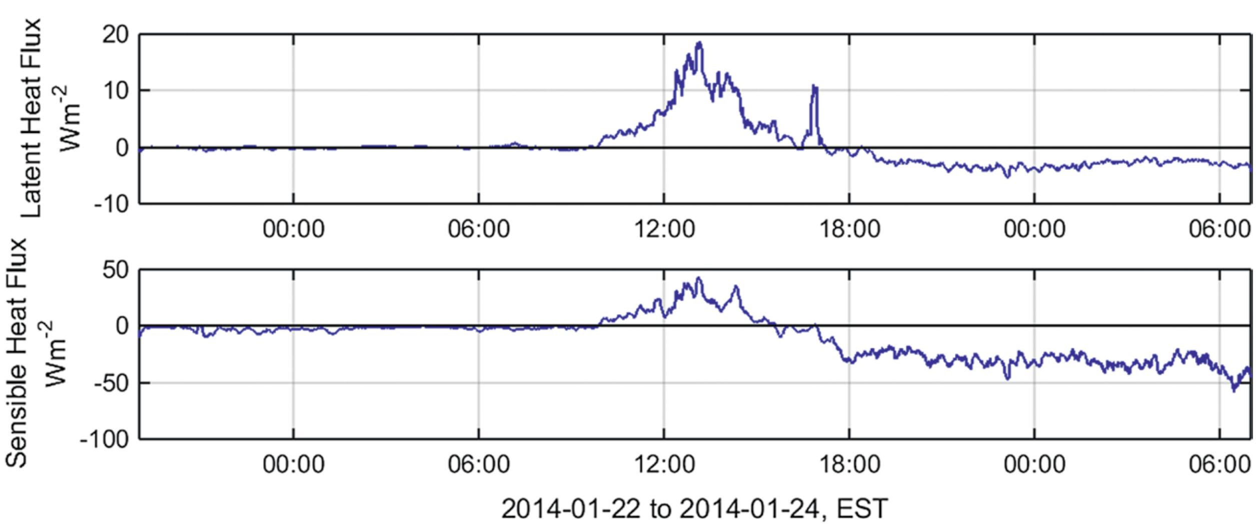

Fig. 5. Time series of MUPS observations of (top) latent and (bottom) sensible heat flux. The fluxes have been smoothed to 5-min running means. These data were collected from about 1900 EST 22 Jan 2014 to about 0700 EST 24 Jan 2014 (a time period that includes IOP 18 and part of IOP 19).

plume. UWKA observations are being exploited to document the structure and dynamics of the individual convective cells and the thermodynamic and kinematic environment in which they form. DOW and Geostationary Operational Environmental Satellite (GOES) imagery are being used to examine the convective field. Weather Research and Forecasting (WRF) Model reanalysis using OWLeS observations is providing the 4D thermal advection and diabatic heating fields necessary to fully explore the boundary layer destabilization mechanisms. MUPS observations are also being employed to describe the surface forcing.

Influence of upwind lakes. Most large field projects on LeSs were previously conducted over the western Great Lakes (e.g., Braham and Kelly 1982; Kristovich et al. 2000). The OWLeS' focus on Lake Ontario provided the unique opportunity to examine the influences of large upwind lakes on LeS evolution over downwind lakes. Lake-effect cloud bands originating from several other Great Lakes commonly extend over Lake Ontario (e.g., Byrd et al. 1991; Sousounis and Mann 2000), which is a distinction also shared with Lake Erie (Rodriguez et al. 2007). IOPs 18 and 23 during OWLeS were conducted to observe the influences of Georgian Bay and Lake Erie, respectively, on LeSs over Lake Ontario. Initial investigations indicate that during IOP 18 snow particles from Georgian Bay lake-effect snows and higher-level clouds overspread the Lake Ontario lake-effect clouds, possibly resulting in natural cloud seeding. During IOP 23, OWLeS and operational observations revealed a mesoscale plume of lake-modified boundary layer air extending northeastward from Lake Erie that enhanced the lake-effect snowstorm over Lake Ontario (as seen in the cloud patterns shown in Fig. 6).

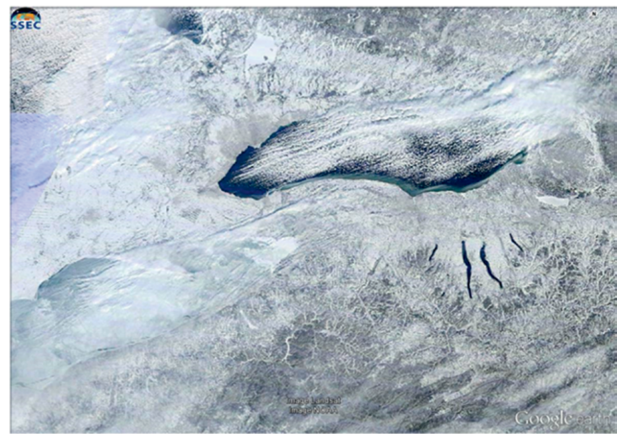

Fig. 6. ***Terra*** **MODIS visible imagery taken at 1548 UTC 28 Jan 2014 (IOP 23), showing bands of lake-effect clouds extending northeastward from Lake Erie toward Lake Ontario.**

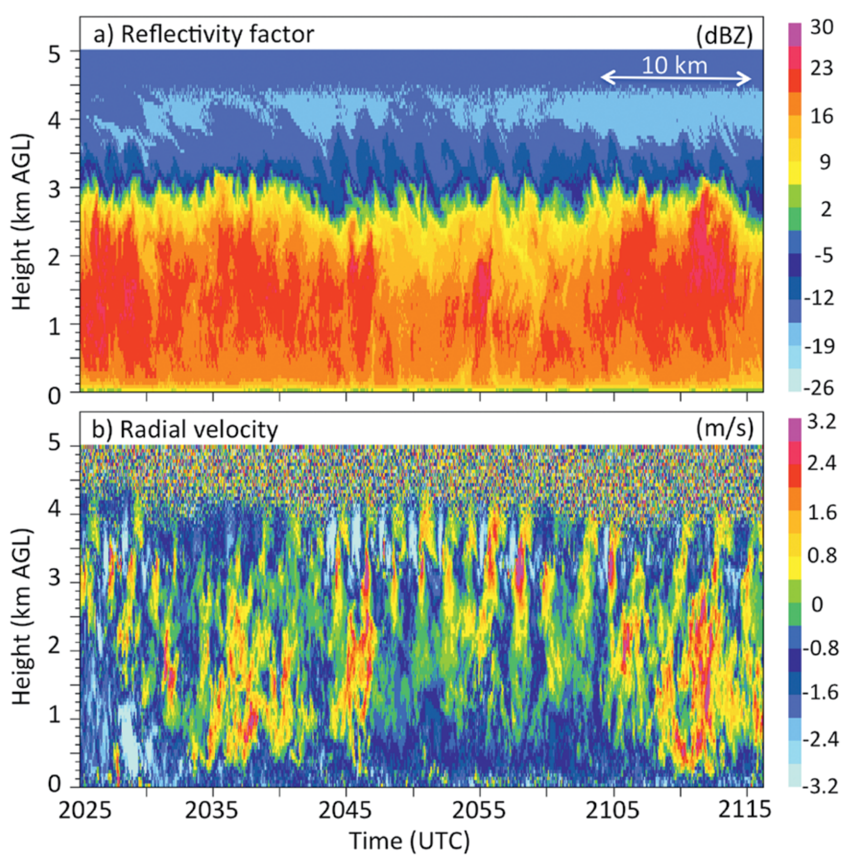

Fig. 7. Time–height sections of vertically pointing (a) reflectivity factor and (b) radial velocity (vertical particle velocity, which is the sum of the vertical air motion and particle terminal fall speed) from the XPR on 11 Dec 2013 (IOP 2b). During this time interval, vertical motion oscillations having a period of about 2 min were sampled within a weak reflectivity region above the tops of convective turrets extending to about 3.2 km AGL. Echo top (−16-dB*Z* contour) extended to about 4.5 km. The mean flow as measured by the 915-MHz wind profiler ranged from 12 m s^{-1} at 170 m to 18 m s^{-1} near 2.5 km. The 10-km horizontal scale in the upper right is based on a mean in-cloud speed of 15 m s^{-1}.

Lake-effect snowstorms developing over the Finger Lakes also experience the effects of an upwind lake, Lake Ontario. Field facilities deployed during OWLeS provided the first known in situ observations of the structure of both lake-effect snowbands over Seneca and Cayuga Lakes, as well as upwind atmospheric conditions between Lake Ontario and the Finger Lakes.

Cloud-scale circulations. The MIPS XPR and the airborne WCR often encountered finescale circulations near the cloud tops of the LLAP bands during OWLeS. An example of such circulations from IOP 2b observed by the MIPS XPR is shown in Fig. 7. At a height of ~3 km, the top of the well-mixed layer, turrets containing hydrometeors lofted at ~2–3 m s^{-1} interspersed with downdrafts with reduced reflectivity, according to XPR time series. The regular spacing between these turrets, with a period of about 2 min, suggests that they are triggered by gravity waves or convective waves in the stable air above (e.g., Melfi and Palm 2012). Kelvin–Helmholtz instability cannot be ruled out, especially given the close proximity of the updrafts and downdrafts in Fig. 7b and the curling appearance of some echo tops in Fig. 7a. The strong cloud-top updrafts suggest that the turrets are due to potential instability release in the residual layer advected over a stabilizing shallow layer over land, downwind of the lake. Indeed, WCR data from several flights indicate that these "generating cells" are confined to land, rather than offshore. They are reminiscent of those documented near the cloud top of mature frontal systems (Rauber et al. 2015).

EDUCATION AND OUTREACH.

Forecasting experience. In support of the OWLeS field project, the National Weather Service (NWS) offices in Binghamton, New York, and Buffalo provided daily lake-effect snowstorm forecasts. These forecasts were given at the beginning of weather briefings, which typically occurred around 1800 UTC [1300 eastern standard time (EST)]. Of particular importance to anticipated or ongoing IOPs was the structure of lake-effect snowbands, as well as their expected locations, strength, persistence, and inland extent, over the following 24–48 h.

These forecasts were complemented by those produced by three rotating groups of undergraduate students, each of which was supervised by a principal investigator (PI). Students examined a variety of observational and model data to make their forecasts, including the operational suite of models run by NCEP, as well as a variety of locally produced convection-allowing models run by universities and local NWS offices. As a part of this forecasting experience, students considered various model solutions for the timing, placement, and type of LeS and were exposed to model discrepancies that were significant at times. The student teams typically presented their forecasts at the daily briefings and led the discussions during off-time briefings or when NWS personnel were not available. Furthermore, the students benefitted from viewing scientific tools and techniques utilized by the more experienced NWS meteorologists.

Several OWLeS scientists later commented that detailed information provided in these forecasts of the likely timing and location of lake-effect precipitation was useful in the planning and prepositioning of critical equipment and field personnel for each IOP.

Student field experiences. Besides being a key part of the OWLeS forecasting activities, students were also heavily involved with operating and maintaining various instruments during the field campaign. In total, 55 undergraduate students and 22 graduate students from eight universities were in the field during OWLeS. Some students spent the majority of their time at fixed sites, while others traveled with mobile sounding units, DOWs, mesonet vehicles, MIPS, mobile snow measurement systems, and the UWKA (Fig. 8).

The largest fixed site was part of the MUPS, based at the Finger Lakes Technical and Career Center (FLTCC) near Stanley, New York. Twenty-two undergraduate students and three graduate students from MU operated MUPS fixed instruments. Similarly, the University of Utah (UU) employed 10 graduate students during portions of the field project, including one from the University at Albany (SUNY-A), at their primary fixed location near North Redfield. There, in addition to operating instruments, the students launched radiosondes. Those students would also travel on a near-daily basis to several other locations to monitor their remote fixed instruments and collect snow measurements.

The large spatial region in which lake-effect snowbands can move onshore necessitated the usage of mobile observation systems. OWLeS benefited from five upper-air sounding units operated by MU, UU, the University of Illinois at Urbana–Champaign (UIUC), the State University of New York at Oswego (SUNY-O), and Hobart and William Smith Colleges (HWS). Besides UU's fixed sounding unit, the four mobile rawinsonde units were typically operated, at least in part, by students. The SUNY-O sounding team included four undergraduate students. Nine undergraduate students were part of the HWS's sounding team. Three undergraduate students, one graduate student, and two staff members assisted with UIUC rawinsonde launches at nearshore locations in southern Ontario, Canada. More than 290 sondes were launched during OWLeS operations. As stressed in the sidebar on field operations in extreme winter weather conditions, students were sometimes traveling with and operating their sounding units during heavy snow, low temperatures, and, in some instances, strong wind conditions.

Students from MU, SUNY-O, and UIUC were assigned to the three DOWs and two mesonet vehicles during OWLeS IOPs. Those students were trained by Center for Severe Weather Research (CSWR) personnel in the operation of the DOWs and mesonet vehicles near the beginning of the OWLeS field campaign. During a typical IOP, each operating DOW was manned by three to four students while each mesonet vehicle was staffed by two to four students. In all, approximately 25–30 students had the unique opportunity of working with CSWR facilities.

Six University of Alabama in Huntsville (UAH) graduate students operated the MIPS. Additionally, 12 SUNY-O undergraduate students routinely traveled to collect surface snow measurements, including unique ice crystal photos, during the OWLeS field campaign. Yet another exciting field experience for students involved their participation in UWKA flight operations. Two graduate students from UU and UW and 14 undergraduate students from MU, SUNY-O, and HWS were aboard various UWKA flights. Duties on those flights were to monitor UWKA radar and lidar data and report, as needed, to the flight scientist, and to serve as the primary UWKA contact with ground crews.

Some particularly interesting experiences of the students participating in OWLeS include the following:

Fig. 8. Photos of students (a) launching a helium-filled kite (Helikite), (b) launching a radiosonde, (c) taking surface snow observations, and (d) servicing an instrumented tower during the OWLeS field operations. [Photos in (a),(d) were taken by R. Clark, MU, and those in (b),(c) by J. Steenburgh, UU.]

- Winds were so extreme during IOP 7 that a sonde was ripped from the hands of SUNY-O and HWS students and blew horizontally into a tree a few hundred feet away.
- One of the students, a ski patroller at Alta ski area in northern Utah (average annual snowfall of 1250 cm) commented that she had never seen it snow as hard as it does on Tug Hill.
- Students encamped in a trailer in Canada experienced indoor rain as water vapor from their breathing created a frozen layer on the roof and sides and then melted as a portable heater warmed the interior.
- During IOP 7, SUNY-O students were stranded at Henderson Harbor, New York, for several hours because of extremely low visibility.

OWLeS open house and K–12 outreach. At the beginning of the OWLeS field operations, an open house was held at the Penn Yan Airport hangar (Penn Yan, New York) in order to introduce the local community to the science, instrumentation, and personnel of the OWLeS project. Introductory presentations on the project objectives by an NSF representative, the lead scientist, and facility providers were followed by tours of the NSF facilities (UWKA and DOWs) and the various university-provided instruments. Students involved with the project helped with the tours and answered questions. Advertising for this event through media, airport personnel, and local universities resulted in a turnout of over 200 people, including local media, local school groups, and members of the surrounding communities.

Throughout the project, numerous outreach events were coordinated with local kindergarten through twelfth grade (K–12) schools on days when the weather did not favor operations. For example,

FIELD OPERATIONS IN EXTREME WINTER WEATHER CONDITIONS

The snowstorms observed during OWLeS are likely among the most intense sampled during a major field campaign. The operating conditions for all teams were exceptionally difficult, and safety concerns were ever present. There were many challenges for the UWKA on the ground, on the runway, and in the air. The DOW crews operated many hours in heavy snowfall, sometimes in blizzard conditions, and often deep into the night. All vehicles suffered more than the normal wear and tear and the MIPS trailer required a major repair (replacement of an entire axle). Sounding teams and snow crystal photography teams spent many hours outside in heavy snow and low-wind-chill conditions. At times, operations were modified for safety reasons. For example, sounding and snow measurement teams elected not to travel to preferred measurement locations on several occasions because of poor road conditions (Fig. SB1).

Safety activities and liability issues related to field operations were discussed prior to the field campaign, prior to IOPs, and during operations. Although a component of planning meetings and personal discussions, each PI ultimately oversaw safety activities for their group given the diversity of organizations and equipment involved in the program. Such activities included education about winter driving and survival prior to leaving for the field, regular checks and briefings prior to IOPs, and the placement of emergency kits in vehicles (e.g., sleeping bags, shovels, flares, first-aid kits).

The summary of safety and liability issues for field trips and courses in the geosciences by Whitmeyer and Mogk (2013) proved useful for safety planning during OWLeS. To our knowledge, no such summary exists for the atmospheric sciences. Atmospheric field campaigns offer unique safety issues related to severe weather, extended operations beyond normal duty cycles, overnight operations, and, for winter campaigns, travel on snow- or ice-covered roads. A community effort to develop field-program safety guidelines, including those conducted in winter environments, could prove beneficial and help limit risk in the future.

Fig. SB1. Photo illustrating dangerous road conditions during OWLeS. (Photos courtesy of R. Clark.)

MU hosted over 100 K–12 students and their teachers at their FLTCC location on eight separate occasions, providing introductory presentations and tours of their instrumentation. The UU students and CSWR personnel visited Sandy Creek's Central School, a rural K–12 district serving areas east of Lake Ontario and portions of Tug Hill, as well as the Pulaski High School in Pulaski, New York, which similarly services areas east of Lake Ontario and portions of Tug Hill. As part of their outreach, they provided lectures, an opportunity to take snow measurements and crystal observations, and tours of a DOW.

CONCLUSIONS. The OWLeS field project collected an unprecedented set of observations of LeSs in the eastern Great Lakes region. Analyses of these data, in combination with numerical simulation studies, will improve our understanding of LeSs and ultimately lead to improvements in LeS forecasting. More than 75 undergraduate and graduate students participated in the field operations, providing unique knowledge and experience with field work in atmospheric sciences.

While the emphasis of the OWLeS field campaign was on LeSs, results of ongoing analyses should impact many other fields and atmospheric phenomena that are not well understood, such as Arctic mixed-phase clouds, polarimetric estimates of precipitation type and intensity, mesoscale circulations generated by complex nonuniform surfaces, boundary layer responses to cloud and precipitation development, and lightning during winter storms.

ACKNOWLEDGMENTS. We greatly appreciate the participation of a large number of students, volunteers, facilities managers, and staff for MIPS, MUPS, DOWs, and UWKA, and weather forecasters from the Buffalo and Binghamton NOAA/NWS Forecast Offices. Particular thanks go to Michael Evans, Michael Jurewicz, and David Zaff. OWLeS was funded by the National Science Foundation, Grants NSF AGS 12 59004 and 12 59257 (both UIUC), 12 58894 (SUNY-O), 12 58548 (HWS), 12 58856 (UW), 12 59020 (MU), 12 58860 (UAH), 12 62090 (UU), 12 59011 (PSU), and 12 59185 (CSWR). The DOWs are NSF-sponsored national facilities funded by NSF Grant AGS 13 61237. Participation of several UU graduate students was made possible with the support of the UU Edward J. Zipser Endowed Research Fund. Participation of the SUNY-A PI and student were funded by a University at Albany Faculty Research Award Program grant. Thanks to both SUNY Oswego and Hobart and William Smith Colleges for hosting research labs and operations centers where project personnel could meet and review data during the OWLeS field campaign. Provision, hosting, or operation of instrumentation is acknowledged from Ron Smith (Yale University, for use of MRR), Carol Yerdon, Jim and Cindy Cheney, John and Cheryl Cheney, Gerhardt and Diane Brosch, Jason and Alix Kowalczyk, Sharon Kristovich, Paul Francia, the Sandy Creek Central School,Curt Morris at Darlington Provincial Park, Paul Gauthier at the City of Cobourg, and Jim Millar and John Martinello at the City of Brighton, Ontario. Phil Bergmaier, Dan Welsh, Yonggang Wang, Luke Bard, Leslie Stoecker, and Ted Letcher assisted in preparing the figures presented here. Beth Hall (ISWS) reviewed this manuscript. Opinions presented in this article are those of the authors and not necessarily those of the funding agencies or their affiliated institutions.

REFERENCES

Agee, E. M., and M. L. Hart, 1990: Boundary layer and mesoscale structure over Lake Michigan during a wintertime cold air outbreak. *J. Atmos. Sci.*, **47**, 2293–2316, doi:10.1175/1520-0469(1990)047<2293:BLAMSO>2.0.CO;2.

Alcott, T. I., and W. J. Steenburgh, 2013: Orographic influences on a Great Salt Lake–effect snowstorm. *Mon. Wea. Rev.*, **141**, 2432–2450, doi:10.1175/MWR-D-12-00328.1.

——, ——, and N. F. Laird, 2012: Great Salt Lake–effect precipitation: Observed frequency, characteristics, and associated environmental factors. *Wea. Forecasting*, **27**, 954–971, doi:10.1175/WAF-D-12-00016.1.

Ballentine, R. J., A. J. Stamm, E. E. Chermack, G. P. Byrd, and D. Schleede, 1998: Mesoscale model simulation of the 4–5 January 1995 lake-effect snowstorm. *Wea. Forecasting*, **13**, 893–920, doi:10.1175/1520-0434(1998)013<0893:MMSOTJ>2.0.CO;2.

Bergmaier, P. T., and B. Geerts, 2016: Airborne radar observations of lake-effect snow bands over the New York Finger Lakes. *Mon. Wea. Rev.*, **144**, 3895–3914, doi:10.1175/MWR-D-16-0103.1.]

Bluestein, H. B., M. M. French, I. PopStefanija, R. T. Bluth, and J. B. Knorr, 2010: A mobile phased-array Doppler radar for the study of severe convective storms. *Bull. Amer. Meteor. Soc.*, **91**, 579–600, doi:10.1175/2009BAMS2914.1.

Braham, R. R., Jr., 1990: Snow particle spectra in lake effect snows. *J. Appl. Meteor.*, **29**, 200–207, doi:10.1175/1520-0450(1990)029<0200:SPSSIL>2.0.CO;2.

——, and R. D. Kelly, 1982: Lake-effect snow storms on Lake Michigan, U.S.A. *Cloud Dynamics*, E. M. Agee and T. Asai, Eds., D. Reidel, 87–101.

——, and D. A. R. Kristovich, 1996: On calculating the buoyancy of cores in a convective boundary layer. *J. Atmos. Sci.*, **53**, 654–658, doi:10.1175/1520-0469(1996)053<0654:OCTBOC>2.0.CO;2.

Burt, C. C., 2007: *Extreme Weather: A Guide & Record Book*. W. W. Norton, 304 pp.

Byrd, G. P., R. A. Anstett, J. E. Heim, and D. M. Usinski, 1991: Mobile sounding observations of lake-effect snowbands in western and central New York. *Mon. Wea. Rev.*, **119**, 2323–2332, doi:10.1175/1520-0493(1991)119<2323:MSOOLE>2.0.CO;2.

Campbell, L. S., W. J. Steenburgh, P. G. Veals, T. W. Letcher, and J. R. Minder, 2016: Lake-effect mode and precipitation enhancement over the Tug Hill Plateau during OWLeS IOP2b. *Mon. Wea. Rev.*, 144, 1729–1748, doi:10.1175/MWR-D-15-0412.1.

Chang, S. S., and R. R. Braham Jr., 1991: Observational study of a convective internal boundary layer of Lake Michigan. *J. Atmos. Sci.*, **48**, 2265–2279, doi:10.1175/1520-0469(1991)048<2265:OSOACI>2.0.CO;2.

Cordeira, J. M., and N. F. Laird, 2008: The influence of ice cover on two lake-effect snow events over Lake Erie. *Mon. Wea. Rev.*, **136**, 2747–2763, doi:10.1175/2007MWR2310.1.

Drennan, W. M., J. A. Zhang, J. R. French, C. McCormick, and P. G. Black, 2007: Turbulent fluxes in the hurricane boundary layer. Part II: Latent heat flux. *J. Atmos. Sci.*, **64**, 1103–1115, doi:10.1175/JAS3889.1.

Hjelmfelt, M. R., 1990: Numerical study of the influence of environmental conditions on lake-effect snowstorms over Lake Michigan. *Mon. Wea. Rev.*, **118**, 138–150, doi:10.1175/1520-0493(1990)118<0138:NSOTIO>2.0.CO;2.

——, 1992: Orographic effects in simulated lake-effect snowstorms over Lake Michigan. *Mon. Wea. Rev.*, **120**, 373–377, doi:10.1175/1520-0493(1992)120<0373:OEISLE>2.0.CO;2.

Inoue, H. Y., and Coauthors, 2011: Finescale Doppler radar observation of a tornado and low-level misocyclones within a winter storm in the Japan Sea coastal region. *Mon. Wea. Rev.*, **139**, 351–369, doi:10.1175/2010MWR3247.1.

Kosiba, K. A., P. Robinson, P. W. Chan, and J. Wurman, 2014: Wind field of a nonmesocyclone anticyclonic tornado crossing the Hong Kong International Airport. *Adv. Meteor.*, 2014, 597378, doi:10.1155/2014/597378.

Kristovich, D. A. R., and R. R. Braham Jr., 1998: Mean profiles of moisture fluxes in snow-filled boundary layers. *Bound.-Layer Meteor.*, **87**, 195–215, doi:10.1023/A:1000836401204.

——, and N. F. Laird, 1998: Observations of widespread lake-effect cloudiness: Influences of lake surface temperature and upwind conditions. *Wea. Forecasting*, **13**, 811–821, doi:10.1175/1520-0434(1998)013<0811:OOWLEC>2.0.CO;2.

——, ——, M. R. Hjelmfelt, R. G. Derickson, and K. A. Cooper, 1999: Transitions in boundary layer meso-γ convective structures: An observational case study. *Mon. Wea. Rev.*, **127**, 2895–2909, doi:10.1175/1520-0493(1999)127<2895:TIBLMC>2.0.CO;2.

——, and Coauthors, 2000: The Lake-Induced Convective Experiment of the Snowband Dynamics Project. *Bull. Amer. Meteor. Soc.*, **81**, 519–542, doi:10.1175/1520-0477(2000)081<0519:TLCEAT>2.3.CO;2.

——, N. F. Laird, and M. R. Hjelmfelt, 2003: Convective evolution across Lake Michigan during a widespread lake-effect snow event. *Mon. Wea. Rev.*, **131**, 643–655, doi:10.1175/1520-0493(2003)131<0643:CEALMD>2.0.CO;2.

Kunkel, K. E., N. E. Westcott, and D. A. R. Kristovich, 2002: Effects of climate change on heavy lake-effect snowstorms near Lake Erie. *J. Great Lakes Res.*, **28**, 521–536, doi:10.1016/S0380-1330(02)70603-5.

Kusunoki, K., M. Murakami, M. Hoshimoto, N. Orikasa, Y. Yamada, H. Mizuno, K. Hamazu, and H. Watanabe, 2004: The characteristics and evolution of orographic snow clouds under weak cold advection. *Mon. Wea. Rev.*, **132**, 174–191, doi:10.1175/1520-0493(2004)132<0174:TCAEOO>2.0.CO;2.

Laird, N. F., D. A. R. Kristovich, X. Z. Liang, R. W. Arritt, and K. Labas, 2001: Lake Michigan lake breezes: Climatology, local forcing, and synoptic environment. *J. Appl. Meteor.*, **40**, 409–424, doi:10.1175/1520-0450(2001)040<0409:LMLBCL>2.0.CO;2.

——, ——, and J. E. Walsh, 2003: Idealized model simulations examining the mesoscale structure of winter lake-effect circulations. *Mon. Wea. Rev.*, **131**, 206–221, doi:10.1175/1520-0493(2003)131<0206:IMSETM>2.0.CO;2.

——, R. Sobash, and N. Hodas, 2009: The frequency and characteristics of lake-effect precipitation events associated with the New York State Finger Lakes. *J. Appl. Meteor. Climatol.*, **48**, 873–886, doi:10.1175/2008JAMC2054.1.

——, ——, and N. Hodas, 2010: Climatological conditions of lake-effect precipitation events associated with the New York State Finger Lakes. *J. Appl. Meteor. Climatol.*, **49**, 1052–1062, doi:10.1175/2010JAMC2312.1.

Maahn, M., and P. Kollias, 2012: Improved Micro Rain Radar snow measurements using Doppler spectra post-processing. *Atmos. Meas. Tech.*, **5**, 2661–2673, doi:10.5194/amt-5-2661-2012.

Magono, C., K. Kikuchi, T. Kimura, S. Tazawa, and T. Kasai, 1966: A study on the snowfall in the winter monsoon season in Hokkaido with special reference to low land snowfall. *J. Fac. Sci. Hokkaido Univ. Ser.*, **7** (11), 287–308.

Melfi, S. H., and S. P. Palm, 2012: Estimating the orientation and spacing of midlatitude linear convective boundary layer features: Cloud streets. *J. Atmos. Sci.*, **69**, 352–364, doi:10.1175/JAS-D-11-070.1.

Miles, N. L., and J. Verlinde, 2005: Observations of transient linear organization and nonlinear scale interactions in lake-effect clouds. Part II: Nonlinear scale interactions. *Mon. Wea. Rev.*, **133**, 692–706, doi:10.1175/MWR-2880.1.

Minder, J. R., T. W. Letcher, L. S. Campbell, P. G. Veals, and W. J. Steenburgh, 2015: The evolution of lake-effect convection during landfall and orographic uplift as observed by profiling radars. *Mon. Wea. Rev.*, **143**, 4422–4442, doi:10.1175/MWR-D-15-0117.1.

MRCC, 2015: Midwest climate watch. Midwestern Regional Climate Center. [Available online at http://mrcc.isws.illinois.edu/cliwatch.]

Niziol, T. A., W. R. Snyder, and J. S. Waldstreicher, 1995: Winter weather forecasting throughout the eastern United States. Part IV: Lake-effect snow. *Wea. Forecasting*, **10**, 61–77, doi:10.1175/1520-0434(1995)010<0061:WWFTTE>2.0.CO;2.

NRCC, 2015: Northeastern Regional Climate Center. [Available online at www.nrcc.cornell.edu.]

NWS, 2015: Lake effect summary: November 17–19, 2014. NWSFO, Buffalo, NY. [Available online at www.weather.gov/buf/lake1415_stormb.html.]

Pazmany, A., R. McIntosh, R. Kelly, and G. Vali, 1994: An airborne 95 GHz dual-polarized radar for cloud studies. *IEEE Trans. Geosci. Remote Sens.*, **32**, 731–739, doi:10.1109/36.298002.

Peters, G., B. Fischer, and T. Andresson, 2002: Rain observations with a vertically looking Micro Rain Radar (MRR). *Boreal Environ. Res.*, **7**, 353–362.

Rao, G. S., and E. M. Agee, 1996: Large eddy simulation of turbulent flow in a marine convective boundary layer with snow. *J. Atmos. Sci.*, **53**, 86–100, doi:10.1175/1520-0469(1996)053<0086:LESOTF>2.0.CO;2.

Rauber, R. M., and Coauthors, 2015: The role of cloud-top generating cells and boundary layer circulations in the finescale radar structure of a winter cyclone over the Great Lakes. *Mon. Wea. Rev.*, **143**, 2291–2318, doi:10.1175/MWR-D-14-00350.1.

Rodriguez, Y., D. A. R. Kristovich, and M. R. Hjelmfelt, 2007: Lake-to-lake cloud bands: Frequencies and locations. *Mon. Wea. Rev.*, **135**, 4202–4213, doi:10.1175/2007MWR1960.1.

Saito, K., M. Murakami, T. Matsuo, and H. Mizuno, 1996: Sensitivity experiments on the orographic snowfall over the mountainous region of northern Japan. *J. Meteor. Soc. Japan*, **74**, 797–813.

Schmidlin, T. W., 1993: Impacts of severe winter weather during December 1989 in the Lake Erie snowbelt. *J. Climate*, **6**, 759–767, doi:10.1175/1520-0442(1993)006<0759:IOSWWD>2.0.CO;2.

Schroeder, J. J., D. A. R. Kristovich, and M. R. Hjelmfelt, 2006: Boundary layer and microphysical influences of natural cloud seeding on a lake-effect snowstorm. *Mon. Wea. Rev.*, **134**, 1842–1858, doi:10.1175/MWR3151.1.

Sousounis, P. J., and J. M. Fritsch, 1994: Lake-aggregate mesoscale disturbances. Part II: A case study of the effects on regional and synoptic-scale weather systems. *Bull. Amer. Meteor. Soc.*, **75**, 1793–1811, doi:10.1175/1520-0477(1994)075<1793:LAMDPI>2.0.CO;2.

——, and G. E. Mann, 2000: Lake-aggregate mesoscale disturbances. Part V: Impacts on lake-effect precipitation. *Mon. Wea. Rev.*, **128**, 728–745, doi:10.1175/1520-0493(2000)128<0728:LAMDPV>2.0.CO;2.

Steiger, S. M., R. Hamilton, J. Keeler, and R. E. Orville, 2009: Lake-effect thunderstorms in the lower Great Lakes. *J. Appl. Meteor. Climatol.*, **48**, 889–902, doi:10.1175/2008JAMC1935.1.

——, and Coauthors, 2013: Circulations, bounded weak echo regions, and horizontal vortices observed within long-lake-axis-parallel–lake-effect storms by the Doppler on Wheels. *Mon. Wea. Rev.*, **141**, 2821–2840, doi:10.1175/MWR-D-12-00226.1.

Tug Hill Commission, 2015: Environment & economy. [Available online at www.tughill.org/environment-economy/.]

Veals, P. G., and W. J. Steenburgh, 2015: Climatological characteristics and orographic enhancement of lake-effect precipitation east of Lake Ontario and over the Tug Hill Plateau. *Mon. Wea. Rev.*, **143**, 3591–3609, doi:10.1175/MWR-D-15-0009.1.

Wang, Z., and Coauthors, 2012: Single aircraft integration of remote sensing and in situ sampling for the study of cloud microphysics and dynamics. *Bull. Amer. Meteor. Soc.*, **93**, 653–668, doi:10.1175/BAMS-D-11-00044.1.

Welsh, D., B. Geerts, J. Minder, J. Steenburgh, P. Bergmaier, X. Jing, and L. Campbell, 2016: Understanding heavy lake-effect snowfall: the vertical structure of radar reflectivity in a deep snowband over and downwind of Lake Ontario. *Mon. Wea. Rev.*, **144**, 4221–4244. doi:10.1175/MWR-D-16-0057.1.]

Whitmeyer, S. J., and D. W. Mogk, 2013: Safety and liability issues related to field trips and field courses. *Eos, Trans. Amer. Geophys. Union*, **94**, 349–351, doi:10.1002/2013EO400002.

Wurman, J., 2002: The multiple-vortex structure of a tornado. *Wea. Forecasting*, **17**, 473–505, doi:10.1175/1520-0434(2002)017<0473:TMVSOA>2.0.CO;2.

——, J. Straka, E. Rasmussen, M. Randall, and A. Zahrai, 1997: Design and deployment of a portable, pencil-beam, pulsed, 3-cm Doppler radar. *J. Atmos. Oceanic Technol.*, **14**, 1502–1512, doi:10.1175/1520-0426(1997)014<1502:DADOAP>2.0.CO;2.

——, K. Kosiba, and P. Robinson, 2013: In situ, Doppler radar, and video observations of the interior structure of a tornado and the wind-damage relationship. *Bull. Amer. Meteor. Soc.*, **94**, 835–846, doi:10.1175/BAMS-D-12-00114.1.

——, ——, ——, and T. Marshall, 2014: The role of multiple-vortex tornado structure in causing storm researcher fatalities. *Bull. Amer. Meteor. Soc.*, **95**, 31–45, doi:10.1175/BAMS-D-13-00221.1.

Yang, Q., and B. Geerts, 2006: Horizontal convective rolls in cold air over water: Buoyancy characteristics of coherent plumes detected by an airborne radar. *Mon. Wea. Rev.*, **134**, 2373–2396, doi:10.1175/MWR3203.1.

Yeager, K. N., W. J. Steenburgh, and T. I. Alcott, 2013: Contributions of lake-effect periods to the cool-season hydroclimate of the Great Salt Lake basin. *J. Appl. Meteor. Climatol.*, **52**, 341–362, doi:10.1175/JAMC-D-12-077.1.

Young, G. S., B. K. Cameron, and E. E. Hebble, 2000: Observations of the entrainment zone in a rapidly entraining boundary layer. *J. Atmos. Sci.*, **57**, 3145–3160, doi:10.1175/1520-0469(2000)057<3145:OOTEZI>2.0.CO;2.

——, D. A. R. Kristovich, M. R. Hjelmfelt, and R. C. Foster, 2002: Rolls, streets, waves, and more: A review of quasi-two-dimensional structures in the atmospheric boundary layer. *Bull. Amer. Meteor. Soc.*, **83**, 997–1001, doi:10.1175/1520-0477(2002)083<0997:RSWAMA>2.3.CO;2.